PHYSICAL REVIEW B VOLUME 2, NUMBER 5 1 SEPTEMBER 1970

Nuclear Magnetic Resonance in $PtSb_2$ and $PtAs_2$

G. T. Mallick, Jr., and P. R. Emtage
Westinghouse Research Laboratories, Pittsburgh, Pennsylvania 15235
(Received 15 December 1969; revised manuscript received 20 April 1970)

The nuclear magnetic resonances of Sb^{121}, Sb^{123}, and Pt^{195} in $PtSb_2$ and $PtAs_2$ are reported. The quadrupole coupling constants e^2qQ/h of Sb are unusually low for compounds of this element, being 98 mHz for Sb^{121} and 124.6 mHz for Sb^{123}; similarly low results have been reported previously for the arsenide. The Pt resonance is anisotropic, with a center of gravity displaced $-0.40\pm0.02\%$ relative to chloroplatinic acid; the shift is probably paramagnetic relative to the bare platinum nucleus. The mean shift and anisotropy are identical in the antimonide and in the arsenide. Analyses of the Sb and As resonances by the method of Townes and Dailey, and also of the anisotropy in the Pt resonance according to Ramsey's theory, all lead to the conclusion that Pt is in the formal valence state (−2) and that all bonds in these compounds are primarily covalent.

I. INTRODUCTION

A. Preliminary

Platinum antimonide is a semiconductor with a narrow band-gap, 0.1 ev, valence-band maxima on the ⟨100⟩ axes, conduction-band minima on the ⟨111⟩ axes, and roughly isotropic effective masses in the neighborhood of 0.2 m. This laboratory's investigations of $PtSb_2$ have for the most part been concerned with its growth and electrical properties[1]; here we report magnetic-resonance studies of this material, together with less complete results on the similar compound $PtAs_2$.

$PtSb_2$ crystallizes in the pyrite structure, which resembles a NaCl lattice with Pt atoms on the Na sites and Sb_2 molecules on the Cl sites. The four Sb_2 pairs in the unit cell have their axes along the four ⟨111⟩ axes. The nearest-neighbor distances are Pt-Sb = 2.68 Å; Sb-Sb = 2.67 Å.

Each Sb site has a nearly tetrahedral environment of three Pt atoms and one Sb atom; the Sb neighbor is in a ⟨111⟩ direction from the site and the surroundings have threefold symmetry about this axis. This configuration of neighbors produces an electric field gradient (efg) at the site, the maximum of $\partial\vec{E}/\partial x$ being along the axis and the asymmetry parameter being zero as a result of the threefold symmetry. Both Sb^{121} and Sb^{123} possess nuclear quadrupole moments and therefore will interact with this efg, the quadrupole interaction is expected *a priori* to be comparable with the Zeeman energy at moderate (~20 kG) magnetic fields.

Each Pt site has six equidistant Sb neighbors on the corners of a distorted octahedron around it; there are four inequivalent sites each with threefold symmetry about one of the ⟨111⟩ axes. The departure of the surroundings from cubic symmery produces an anisotropic shift in the resonance that is small compared with the total chemical shift.

B. Antimony: Quadrupole Interactions

The Hamiltonian of a nucleus of spin I, quadrupole moment Q, and gyromagnetic ratio γ in an electric field gradient eq and magnetic field $\vec{H}$ is

$$H=[e^2qQ/4I(2I-1)][3I_{z'}^2-I(I+1)]-\gamma\hbar\vec{H}\cdot\vec{I} \quad , \quad (1)$$

in which z' is the principal axis of the efg tensor and the asymmetry parameter is taken as zero. For the Sb atoms in $PtSb_2$ the axis z' is one of the ⟨111⟩ directions. It is well known that exact solutions to this Hamiltonian exist only in special cases, one of which is given below.

When the magnetic field $\vec{H}$ is parallel with z' the term involving $\vec{H}$ commutes with the quadrupole part of the Hamiltonian. The energy levels of (1) are then precisely the sum of the quadrupole levels and the Zeeman shift, which is linear in the field. This situation holds for two of the eight Sb atoms when $\vec{H}$ is in a ⟨111⟩ direction, which is the case that we have studied most. The frequencies of the allowed magnetic dipole transitions, $|\Delta m|=1$, are

$$\omega=n\omega_Q\pm\gamma H \quad , \quad (2a)$$

in which

$$\omega_Q\equiv 3e^2qQ/2I(2I-1)\hbar$$

and n is a positive integer or zero.

When the magnetic field makes some angle α with the symmetry axis then general solutions cannot be given; we shall take the low-field case only. For zero asymmetry parameter and low field it is shown by Das and Hahn[2] that when $m\neq\frac{1}{2}$ the solutions are

$$E_m(H)=E_{0|m|}-m\gamma\hbar H\cos\alpha \quad ,$$

m being the magnetic quantum number and $E_{0|m|}$ the quadrupole energy. For transitions that do not involve the quantum number $m = \frac{1}{2}$ one has

$$\omega = n\omega_Q \pm \gamma H \cos\alpha \quad (n \neq 0, 1) \ . \tag{2b}$$

In the case $m = \frac{1}{2}$ the transverse components of $\vec{H}$ link states that are degenerate under the quadrupole interaction alone. The frequencies of allowed transitions involving $|m| = \frac{1}{2}$ are

$$\begin{aligned} \omega_\alpha &= \omega_Q \pm \tfrac{1}{2}(3-f)\gamma H \cos\alpha \ , \\ \omega_\beta &= \omega_Q \pm \tfrac{1}{2}(3+f)\gamma H \cos\alpha \ , \\ \omega_\gamma &= f\gamma H \cos\alpha \ , \end{aligned} \tag{2c}$$

where

$$f = [1 + (I + \tfrac{1}{2})^2 \tan^2\alpha]^{1/2} \ .$$

C. Platinum: Chemical Shift

It has been shown by Bloembergen and Rowland[3] that in surroundings of low symmetry the chemical shift of a resonance depends on the direction of the magnetic field [we take it that a paramagnetic shift σ is positive; i.e., at fixed frequency the field H at which resonance occurs is $H_0/(1+\sigma)$, H_0 being the field at which the bare nucleus resonates; the shift $\Delta H = H - H_0$ then has a sign opposite to that of σ]. In particular, when the surroundings have axial symmetry they find that the shift σ depends only on the angle θ between the axis and the field, and is of the form

$$\sigma = \sigma_0 - \sigma_1(3\cos^2\theta - 1) \ . \tag{3}$$

In Sec. III we show that, for the pyrite structure, the ratio σ_1/σ_0 depends mainly on the degree of deformation of the surrounding octahedron rather than the chemical nature of the neighboring atoms; this expectation is realized for the Pt resonance in $PtSb_2$ and $PtAs_2$.

The symmetry axes for the four Pt sites are the four $\langle 111 \rangle$ directions; the shifts in the field at which resonance occurs when the frequency is held constant are

$$\begin{aligned} &[000] \text{ sublattice:} \quad \Delta H/H_0 = -\sigma_0 + \sigma_1(lm + mn + nl) \ , \\ &[011] \text{ sublattice:} \quad \Delta H/H_0 = -\sigma_0 + \sigma_1(lm - mn - nl) \ , \\ &[101] \text{ sublattice:} \quad \Delta H/H_0 = -\sigma_0 + \sigma_1(-lm + mn - nl) \ , \\ &[110] \text{ sublattice:} \quad \Delta H/H_0 = -\sigma_0 + \sigma_1(-lm - mn + nl) \ , \end{aligned} \tag{4}$$

in which (lmn) are the direction cosines of H referred to crystal coordinates.

In powder samples the line shape results from an average over angles of the individual resonances; a brief recapitulation of Bloembergen and Rowland's description follows. Let the number of atoms resonating at fields between H and $H + dH$ be $n(H)\,dH = N \sin\theta\, d\theta$, in which H and θ are related through $H - H_0 = -\sigma H_0$, σ being given in Eq. (3). Noting that $\sigma \ll 1$, one has

$$\begin{aligned} n(H') = N \sin\theta \frac{d\theta}{dH'} &\sim (H' + \tfrac{1}{2}W)^{-1/2}, \quad -\tfrac{1}{2}W < H' < W \\ &= 0 \qquad\qquad , \text{ elsewhere} \end{aligned}$$

in which $W = 2\sigma_1 H_0$ and H' is measured from the center of gravity of the resonance. It will be noted that $n(H')$ has an integrable pole at $-\frac{1}{2}W$ and a discontinuity at W; these features are smoothed out by the breadth of the individual resonances. If $g(H - H', A)$ is the response to a field H of an individual atom resonating at H' (A being the width of this resonance), then the response of the powder is

$$R(H) = \int_{-W/2}^{W} n(H')g(H - H', A)\,dH' \ , \tag{5}$$

$n(H')$ being given above. These remarks are extended in Appendix B to cover the case in which the intrinsic linewidth A is itself anisotropic, a state of affairs that exists in $PtSb_2$ and exerts a marked effect on the powder pattern.

II. APPARATUS AND OBSERVATIONS

Single crystals used in these experiments were grown from the melt using the Czochralski technique by Damon, Miller, and Sagar.[1] Orientation was accomplished by means of standard Laue back-reflection x-ray photographs. Single crystals used in our experiment were approximately 3mm × 3mm × 10mm. The $PtSb_2$ powder samples were prepared by grinding single crystals. While most of the $PtSb_2$ data was obtained on undoped samples with carrier concentration $n_H \sim 6 \times 10^{18}$, a tin-doped ($n_H \sim 10^{20}$) sample was also used.

The $PtAs_2$ samples were prepared by heating the required amounts of platinum and arsenic in an evacuated Vycor tube to 650 °C, and allowing them to remain at the elevated temperature overnight. The resultant material was then ground and pressed, and the firing process repeated. Three overnight firings were executed, with grinding and pressing to assure the complete reaction of the platinum and the arsenic. The final pellet was then sintered at 1000 °C and crushed again. The $PtAs_2$ powder was studied by x-ray diffraction to assure that no second-phase material was present.

All of the powders used were sifted through a # 200 mesh seive to assure that the size of the particles was smaller than the rf skin depth. A pinch of aluminum powder was mixed with the sample powders to provide a magnetic field calibrator. The Knight shift of aluminum was taken to be 0.162% at liquid-helium temperatures.[4]

The apparatus used to study these resonances was

quite conventional and is shown in block form in Fig. 1. The detector was a marginal oscillator of the Pound-Knight-Watkins type capable of covering the 8.5–16.9-mHz frequency range. The frequency was monitored by a Hewlett-Packard 5245L counter. The samples were placed in the rf coil which comprised the tank circuit of the oscillator. The coil and sample were then immersed in liquid helium contained in a glass Dewar placed between the pole faces of a 12-in. Varian electromagnet with a 1.25-in. air gap. A Kinney KC-8 vacuum pump was capable of lowering the temperature of the bath to 1.57 °K, as measured by He vapor pressure. The magnetic field was controlled by a Varian Mark II Fieldial. Fields as high as 20 kG were attainable in our system. The field was directly plotted against the output of a PAR JB5 lock-in amplifier, displaying the derivative of NMR absorption versus field. Magnetic field modulation as large as 24 G peak to peak (p-p) or as small as 2 G (p-p) were used, depending upon whether we were searching for unknown quadrupole resonances, or carefully studying the details of the Pt line shape.

For the quadrupole studies, the field was calibrated using H^1, Cu^{63}, Cu^{65} (from the rf coil), and Pt^{195} resonances, with γ's taken from the Varian NMR chart. Knight shifts are negligible. We were unable to make measurements below about 250 G, because the Fieldial reacted adversely to the field modulation. Our observed low-field lines, however, were sufficiently linear as to render extrapolation through this region to zero magnetic field quite unambiguous.

In the Pt^{195} line-shape studies, rf levels as low as possible were used, because the line saturated easily. Resonances were always traversed with both increasing and decreasing fields to minimize this effect, and permit us to determine the true line shape. Some degree of saturation was always noted, however.

In reporting the Sb resonance measurements we

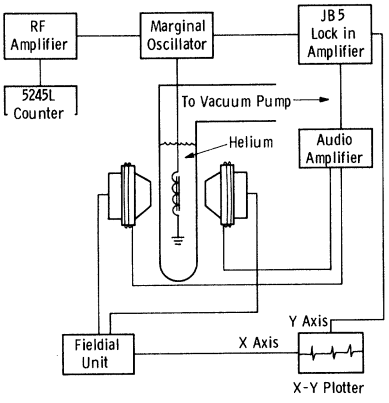

FIG. 1. Block diagram of apparatus.

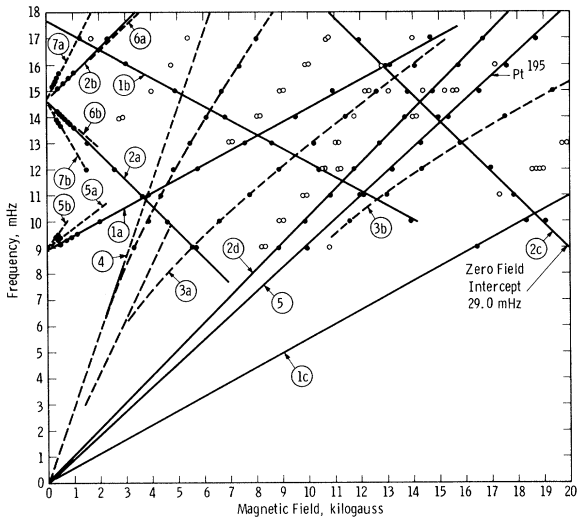

FIG. 2. Resonance positions at fixed frequency as H is varied for fixed frequencies between 9 and 17 mHz. The identification of the various lines is as shown in Table III.

shall consider only the case in which the field is parallel with a ⟨111⟩ direction, since in this case Eq. (2a) holds at all fields for a quarter of the Sb atoms, and some of the resonances can therefore be identified easily. Measurements with fields in the [100] and [110] directions were made and gave the same values for the low-field limits $n\omega_Q$ as did the [111] measurements; interpretation of the lines was, however, not attempted except at the lowest fields, because of the complexity of the spectrum.

Figure 2 shows the observed Sb resonances for $H \parallel \langle 111 \rangle$, the dots being strong resonances and the open circles weak. Solid lines are those given by Eq. (2a) for Sb sites whose symmetry axis is parallel with the field; straight dotted lines are those given by Eqs. (2b) and (2c) for the remaining three quarters of the Sb sites. No serious attempt was made to identify the lines represented by open circles. The dotted lines that go towards the origin, (3a) and (4), are not linear in the field – and are not expected to be – but they approach the calculated (dotted) straight lines sufficiently well for the identification to be made.

The quantities used in calculations to fit the experimental data were

$$\mathrm{Sb}^{121},\ I=\tfrac{5}{2},\quad \mathrm{Sb}^{123},\ I=\tfrac{7}{2}\ ,$$

$$\nu_Q^{121}=14.6\ \mathrm{mHz},\quad \nu_Q^{123}=8.9\ \mathrm{mHz}\ ,$$

$$\gamma^{121}=6.402\times10^3\ \mathrm{HzG^{-1}},\quad \gamma^{123}=3.467\times10^3\ \mathrm{HzG^{-1}}\ ,$$

where $\nu_Q=\omega_Q/2\pi$. The γ's are taken from the Varian NMR table. From the values of ν_Q the coupling constants are readily found, and are

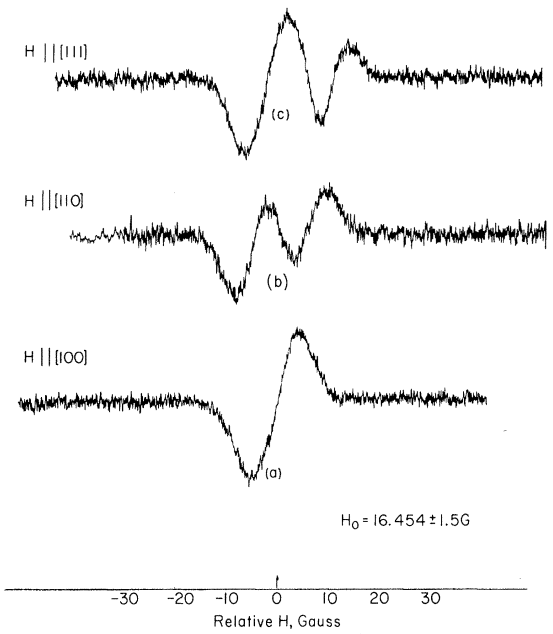

FIG. 3. Single-crystal Pt^{195} resonances in $PtSb_2$, taken at $H_0 = 16.454$ kG, with H_0 parallel to the a [100], b [110], and c [111] crystallographic directions.

$$e^2qQ^{121}/h = 98.0 \text{ mHz}, \quad e^2qQ^{123}/h = 124.6 \text{ mHz}. \quad (6)$$

The ratio of these coupling constants gives $Q^{123}/Q^{121} = 1.28$, in good agreement with Murakawa.[5]

Absorption derivatives for the Pt resonance in single crystals of $PtSb_2$ are shown in Fig. 3 for various field directions; they were taken at 15.000 mHz, and the center of the resonance is $H_0 = 16\,454$ G. As is predicted by Eq. (4) there is only one resonance frequency for $H \parallel [100]$, two resonances of equal magnitude for $H \parallel [110]$, and two resonances whose magnitudes are in the ratio 3:1 for $H \parallel [111]$. The ratio of the [110] splitting to the [111] splitting is 3:4, as given by Eq. (4), and the fact that the stronger resonance is at the lower field in the [111] case shows that σ_1 is positive. Taking chloroplatinic acid, H_2PtCl_6, as standard, the shifts are

$$\sigma_0 = -4.0 \pm 0.2 \times 10^{-3}, \quad \sigma_1 = 3.0 \pm 0.2 \times 10^{-4} \ . \quad (7)$$

Further measurements were made on $PtSb_2$ samples in which the carrier concentration ranged between $< 10^{18}$ and $\sim 10^{20}$ current carriers/cc, and also at temperatures of 1.8 and 77 °K; no changes in the shift were found.

The middle resonance of Fig. 3, $H \parallel [110]$, was studied as a function of field intensity from $H = 10$ kG to $H = 18$ kG; the splitting of the doublet was found to be linear in the field within our ability to measure the separation. The separation of these two lines at 15 mHz was measured as a function of field orientation for fields in the (001) plane; the results are shown in Fig. 4 together with the value found from Eq. (4),

$$\Delta H = 2\sigma_1 H_0 \sin 2\theta = 10 \text{ G} \times \sin 2\theta \ ,$$

θ being the angle the field makes with the [100] axis.

No single crystals of $PtAs_2$ were available, so powder measurements of the Pt resonance in $PtSb_2$ and $PtAs_2$ were made. The results are shown in Fig. 5; circles mark the absorption derivatives calculated from Eq. (5) and Appendix B, the agreement being good. The calculated powder line shape is determined entirely by the single-crystal data for the antimonide; in the arsenide the intrinsic linewidth A was available as a parameter. The values of both the mean shift σ_0 and the anisotropic component σ_1 are the same in the arsenide as in the antimonide, within experimental error. In Ref. 6 we note the intrinsic line shapes and some difficulties in the calculation of the powder line shape.

III. DISCUSSION

A. Prelimary

Most of the ensuing remarks are directed towards the two different bonding schemes that may be used in describing $PtSb_2$ or $PtAs_2$; in these schemes, the charges may be assigned as either $Pt^{4+}Sb_2^{2-}$ or $Pt^{2-}Sb_2^{+}$. The first of these corresponds to ionic bonding between Pt atoms and Sb_2 molecules, the atoms of which are covalently bonded as in the halogens. The second is a generally covalent scheme in which the four electrons remaining on each Sb atom form the usual tetrahedral bonds with its neighbors and each Pt atom forms d^2sp^3 octahe-

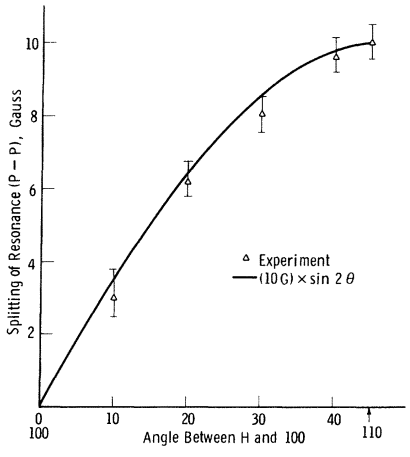

FIG. 4. Separation of doublet observed when H_0 is rotated in a plane perpendicular to a [100] direction. The solid line is predicted from theory, normalized to the splitting observed when H is parallel to [111].

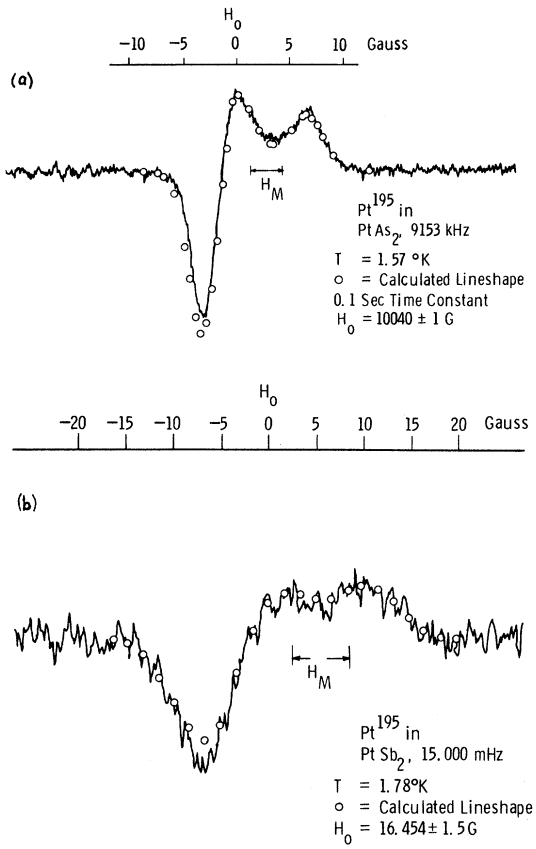

FIG. 5. (a) $Pt^{195}As_2$ powder resonance. (b) $Pt^{195}Sb_2$ powder resonance. Circles are calculated by the methods discussed in Appendix B.

dral bonds. The discussion is cast largely in terms of atomic orbitals, neglecting the difficulties that these may meet in a narrow band-gap material.

B. Sb Resonance

Table I shows values of the quadrupole coupling constant for Sb^{121} and As^{75} in various compounds, including Jones's[7] value for $PtAs_2$ (the list is probably not exhaustive); Sb^{123} has been omitted for simplicity, a practice that will be continued. It is notable that the coupling constant in $PtSb_2$ and $PtAs_2$ is much less than in any other compound of these elements, even though the surroundings are unsymmetrical; the Sb^{121} coupling constant is, in fact, close to that for the elemental metal, which suggests that ionic effects are unimportant and that the charge distribution in the bonds plays the major role. In the following argument we shall consider the antimonide alone and quote similar results for the arsenide at the end.

The quadrupole moment[5] of Sb^{121} is $0.53 \pm 0.10 \times 10^{-24}$ cm^2; from the value of the coupling constant in Eq. (6) the electric field gradient is

$$eq = 2.5 \times 10^{15} \text{ esu} \quad . \tag{8}$$

This gradient is the sum of terms coming from the ionic field and from the nature of the bonds,

$$eq = eq_{\text{ion}} + eq_{\text{bond}} \quad . \tag{9}$$

A given Sb atom has four nearest neighbors; one Sb atom of charge $-\frac{1}{2}ne$ on a [111] axis and three Pt atoms with charges $+ne$ whose directions from the site make an angle $\theta = 100.2°$ with the [111] axis and are symmetrically disposed about that axis; the ionic contribution is

$$eq_{\text{ion}} = -(1+\gamma)e^2 \sum_{n_i} (3\cos^2\theta_i - 1)/r_i^3$$

$$= 1.405n \times 10^{15} \text{ esu} \quad , \tag{10}$$

in which γ is the Sternheimer antishielding factor, $1+\gamma = 15$,[8] and n is the number of positive electronic charges on a Pt atom.

The lack of spherical symmetry of the electron charge in the valence electrons on the atom produces the term eq_{bond} in Eq. (9). If $\rho(\vec{r}) = R(r) \times g(\theta, \phi)$ is the electron density associated with these electrons, then

$$eq_{\text{bond}} = e \int \rho(\vec{r})(3\cos^2\theta - 1) r^{-3} d^3r$$

$$= \tfrac{5}{4}\, eq_{\text{at}} \int g(\theta, \phi)(3\cos^2\theta - 1)\sin\theta \, d\theta \, d\phi \quad , \tag{11}$$

in which eq_{at} is a quantity defined by Townes and Dailey[9] and contains the radial integrals. Its value may be obtained from the fine structure of atomic spectra.

Define the A axis as the axis joining Sb pairs, and three C axes directed towards Pt neighbors at the angle $\theta = 100.2°$ to the A direction. We assume that $\rho(\vec{r})$ comes from orthogonal wave functions pointing in these directions

$$\psi_A = \sqrt{2}\,\psi(s)\cot\theta + [(1 - 3\cos^2\theta)^{1/2}/\sin\theta]\psi(p_z) \quad ,$$

$$\psi_{CI} = [(1 - 3\cos^2\theta)^{1/2}/3^{1/2}\sin\theta]\psi(s)$$

$$+ (\tfrac{2}{3})^{1/2}[\psi(p_z)\cot\theta - \psi(p_x)] \quad ,$$

the other two wave functions being rotations of ψ_{CI} through angles $\pm 120°$ about the A axis. The total electron densities in the three C directions are equal and not necessarily the same as that in the A direction. Denoting these densities by ρ_C and ρ_A, and setting the above wave functions in Eq. (11) one finds

$$eq_{\text{bond}} = eq_{\text{at}}(\rho_A - \rho_C)(1 - 3\cos^2\theta)/\sin^2\theta$$

$$= 31.2(\rho_A - \rho_C) \times 10^{15} \text{ esu} \quad , \tag{12}$$

in which the value $eq_{\text{at}} = 33.74 \times 10^{15}$ esu, given by Barnes and Smith,[10] has been used.

We now use Eqs. (8)–(10), and (12) to find $\rho_A - \rho_C$

TABLE I. Quadrupole energies for As^{75} and Sb^{121} in different compounds.

Material	e^2qQ/h (mHz)	Remarks	Reference
$SbCl_3$	383.66	distorted pyramidal configuration, $\eta \neq 0$	a
$AsCl_3$	157.9		b
Sb_2O_3[c]	554.83	pyramidal configuration, $\eta = 0$	d
As_2O_3[e]	233.56		f
$SbBr_3$	321.92	distorted pyramidal configuration, $\eta \neq 0$	g
$AsBr_3$	122.36		h
Sb_2Pt	98.0	pyrite structure, tetrahedral configuration, $\eta = 0$	This work
As_2Pt	52.96		(Ref. 7)
Sb, metal	76.867	arsenic crystal structure $\eta = 0$	(Ref. 8)

[a] H. G. Dehmelt and H. Kruger, Z. Physik 130, 385 (1951).
[b] R. G. Barnes and P. J. Bray, J. Chem. Phys. 23, 407 (1955).
[c] Senarmonite.
[d] R. G. Barnes and P. J. Bray, J. Chem. Phys. 23, 1177 (1955).
[e] Arsenolite.
[f] H. Kruger and U. Meyer-Berkhout, Z. Physik 132, 221 (1952).
[g] T. C. Wang, Phys. Rev. 99, 566 (1955).
[h] R. G. Barnes and P. J. Bray, J. Chem. Phys. 23, 207 (1955).

for the charge schemes Pt^{4+} and Pt^{2-}. The results are shown in Table II together with values obtained from a similar calculation in the arsenide; for each charge scheme two values of $\rho_A - \rho_C$ are given since the sign of eq is not known. Parameters used in the arsenide calculation are bond angles as in the antimonide; interatomic distance is 2.49 Å; $eq_{at} = 19.75 \times 10^{15}$ esu, from Ref. 10; $Q = 0.3 \times 10^{-24}$ cm^2; coupling constant of Ref. 7. We are not able to find an estimate for $(1+\gamma)$ for As^{75}, we estimate it to be somewhat less than $(1+\gamma)$ Sb^{121}, and accordingly, we arbitrarily take as its value $(1+\gamma)$ $As^{75} = 10$.

The last two columns of Table II are the only ones that are in reasonable agreement with common sense, providing one remembers that the values $\rho_A - \rho_C$ are densities of valence electrons belonging to the Sb atom itself: The first two columns correspond to an electron deficit in the direction of the one covalent bond that the atom forms. The last column corresponds to almost exactly even covalent bonding. This identification, however, is not certain since it is unwise to take a formal charge scheme too seriously; one can say only that the results favor the covalent Pt^{2-} scheme.

C. Pt Resonance

The mean shift in the Pt resonance is -0.40% relative to H_2PtCl_6, the usual standard, and is independent of temperature, carrier concentration, and magnetic field; it is therefore most likely to be a paramagnetic shift of the type treated by Ramsey.[11] According to Drain[12] the shift of the Pt resonance in H_2PtCl_6 is $+0.7\%$ relative to the "bare" platinum nucleus. This estimate is also regarded as realistic by Clogston, Jaccarino, and Yafet.[13] The shift in the antimonide is then indeed paramagnetic, the mean and anisotropic components being

$$\sigma_0(\text{true}) \simeq 3 \times 10^{-3}, \quad \sigma_1 = 3 \times 10^{-4}. \tag{13}$$

Ramsey's formula for the paramagnetic shift is

$$\sigma = \text{const} \sum_{n,k} \frac{\langle 0 | L_{H_k} | n \rangle \langle n | L_{H_k}/r^3 | 0 \rangle}{(E_n - E_0)}, \tag{14}$$

in which $|0\rangle$ is the ground state, $|n\rangle$ an excited state, L_{H_k} is the component parallel to H of the angular momentum operator for the kth electron in the system, and E_n is the energy of the nth state. Use of this formula requires precise knowledge of all pertinent wave functions and several authors[14,15] have discussed the related problem of Co^{3+} in an octahedral crystal field; in particular, Walstedt *et al.*[15] have shown that it may be necessary to allow for the augmentation of molecular orbitals with ligand wave functions in order to obtain the magni-

TABLE II. Calculated values of $\rho_A - \rho_C$, for platinum valence states (+4) and (−2).

	Pt^{+4}	Pt^{-2}
Sb	−0.10, −0.26	+0.17, 0.01
As	−0.12, −0.36	+0.24, −0.01

tude of σ when substantial covalency is present. The problem is much simplified if one seeks to obtain not the magnitude of σ, but its angular dependence, for in this case we can hope to lump all of our ignorance together into a single factor containing the radial integrals and energy denominators.

The surroundings of a Pt atom in $PtSb_2$ are best described as an octahedron compressed along a ⟨111⟩ direction and rotated about it. The description of these surroundings and the construction of appropriate orbitals are given in Appendix A, and it is there shown that for an individual site σ has the form

$$\sigma = \sigma_0[1 - \lambda\alpha^2(3\cos^2\theta - 1)] \ ,$$

$\lambda = +1$ for Pt^{2-} and $\lambda = -\frac{3}{2}$ for Pt^{4+}, θ being the angle between H and the threefold axis of the site, and α being proportional to the distortion of the octahedron, $\alpha^2 = 0.1$. This is just Eq. (3) with $\sigma_1/\sigma_0 = \lambda\alpha^2$; from the values in (13) we have then $\lambda = 1.0$, which is the value calculated for Pt^{2-}. That the ratio σ_1/σ_0 does depend primarily on the crystal structure was confirmed by the breadth of the $PtAs_2$ powder spectrum in Fig. 5, where the calculated points were obtained on the assumption that the ratio was the same as in the antimonide.

That the calculated and observed values of λ agree in magnitude is fortuitous, for the calculated value depends on the rather arbitrary criterion used in constructing deformed octahedral wave functions around the Pt atom. For a given Pt valence state, however, the sign of λ depends only on the requirement that the bonds be distorted in the direction of the distortion of the octahedron, and the observed sign is appropriate to the state Pt^{2-} rather than Pt^{4+}.

We note that the observed mean line breadths, 3.5 G in the antimonide and 1.5 G in the arsenide (see Ref. 6) are much greater than those calculated from magnetic dipole interactions, 1.0 and 0.4 G, respectively; also that they are in the ratio 2.3:1, the dipole moments of Sb and As being in the ratio 2.1:1. Most of the observed second moment probably comes from exchange broadening,[3,16] the anisotropy that is found in the Sb linewidth arising from a pseudodipolar interaction that is expected to be present when exchange broadening is important.

IV. CONCLUSION

Studies of the NMR of Pt and Sb in $PtSb_2$ and $PtAs_2$ have been undertaken. The quadrupole coupling constants of Sb^{121} and Sb^{123} are given in Eq. (6); particular attention is drawn to the small magnitudes that these constants have compared with those in other compounds of Sb and As (see Table I). The isotropic and anisotropic components of the chemical shift of the Pt resonance relative to H_2PtCl_6 are given in Eqs. (7). Equation (13) notes the probable true value of the mean shift which is paramagnetic.

Analysis has proceeded from an atomic-orbital point of view with the end of choosing between two possible bonding schemes for the compound, $Pt^{4+}Sb_2^{2-}$ (mostly ionic bonding) or $Pt^{2-}Sb_2^{+}$ (mostly covalent bonding); conclusions for the antimonide hold also for the arsenide. The quadrupole coupling constant of antimony suggests that platinum is in the state Pt^{2-} rather than Pt^{4+}, but no definite conclusion could be drawn; the anisotropy of the paramagnetic chemical shift in the platinum resonance is compatible only with the state Pt^{2-}. We conclude

TABLE III. Identification of various lines as shown in Fig. 2.

	I	$m_1 <=> m_2$
	H parallel to symmetry axis	
1a:	$I=\frac{7}{2}$	$-\frac{3}{2} <=> -\frac{1}{2}$
1b:	$I=\frac{7}{2}$	$+\frac{5}{2} <=> +\frac{3}{2}$
1c:	$I=\frac{7}{2}$	$+\frac{1}{2} <=> -\frac{1}{2}$
2a:	$I=\frac{5}{2}$	$+\frac{3}{2} <=> +\frac{1}{2}$
2b:	$I=\frac{5}{2}$	$-\frac{3}{2} <=> -\frac{1}{2}$
2c:	$I=\frac{5}{2}$	$+\frac{5}{2} <=> +\frac{3}{2}$
2d:	$I=\frac{5}{2}$	$+\frac{1}{2} <=> -\frac{1}{2}$
	H not parallel to symmetry axis	
3a:	$I=\frac{7}{2}$	$- <=> +$
3b:	$I=\frac{7}{2}$	$-\frac{3}{2} <=> -$ [a]
4 :	$I=\frac{5}{2}$	$- <=> +$
5a:	$I=\frac{7}{2}$	$-\frac{3}{2} <=> -$
5b:	$I=\frac{7}{2}$	$-\frac{3}{2} <=> +$
6a:	$I=\frac{5}{2}$	$-\frac{3}{2} <=> -$ [b]
6b:	$I=\frac{5}{2}$	$+\frac{3}{2} <=> +$ [b]
7a:	$I=\frac{5}{2}$	$-\frac{3}{2} <=> +$
7b:	$I=\frac{5}{2}$	$+\frac{3}{2} <=> -$

[a] Tentative, should go to 8.9 mHz at $H=0$.
[b] Dotted line.

that the system of bonding in these compounds is predominantly covalent rather than the more conventional ionic scheme.

ACKNOWLEDGMENTS

The authors are indebted to Dr. D. H. Damon for supplying the $PtSb_2$ single crystals, to P. Piotrowski for orienting and cutting them, to Miss B. J. Kagle for undertaking the computations, to Dr. R. C. Miller for continuous help and encouragement, and to Dr. A. J. Panson and Dr. J. P. McHugh for many stimulating discussions.

APPENDIX A: EVALUATION OF MATRIX ELEMENTS

We wish to distinguish between the valence states Pt^{+4} and Pt^{-2}; the only matrix elements involved are those connecting states of equal l, and the greatest contribution to the shift comes from terms involving the least energy denominator, so we must try to suggest a rough scheme for the energy levels associated with a Pt atom in the two valence states. Each atom is surround by six Sb atoms, forming a nearly regular octahedron (see below); the d orbitals then split by the crystal field into bonding (d_b) and nonbonding (d_{nb}) sets: $d_b = d_{x^2-y^2}$, $d_{3z^2-r^2}$, and $d_{nb} = d_{xy}$, d_{zy}, d_{zx}. In both valence states, the $5s$ and $5p$ states are filled (see Fig. 6). In Pt^{2-}, the $5d^2 6s 6p^3$ orbitals are engaged in bonding, the $5d_{nb}$ orbital being the highest occupied level. The lowest empty levels are the $6d$ states, with the $6d_b$ states being lower in energy than the $6d_{nb}$ states as a result of the crystal field. In Pt^{4+} the bonding is wholly ionic, and the filled $5d_{nb}$ states lie below the empty $5d_b$ states. The most important transitions in Eq. (14) are marked with arrows; in both cases the least energy denominator is between d_b and d_{nb} states, so the two cases cannot be distinguished unless the crystal-field splitting of the $6d$ states in Pt^{2-} is small compared with the $5d$-$6d$ energy difference. In the following we shall suppose

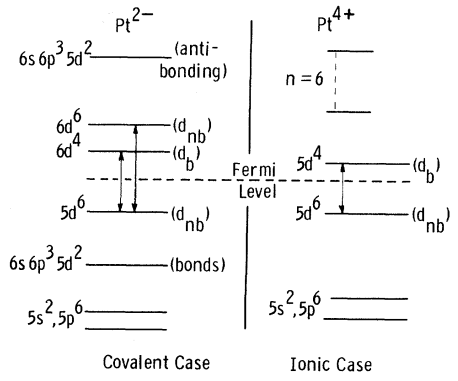

FIG. 6. Energy-level diagrams for Pt^{-2} and Pt^{+4} in the octahedral crystal field.

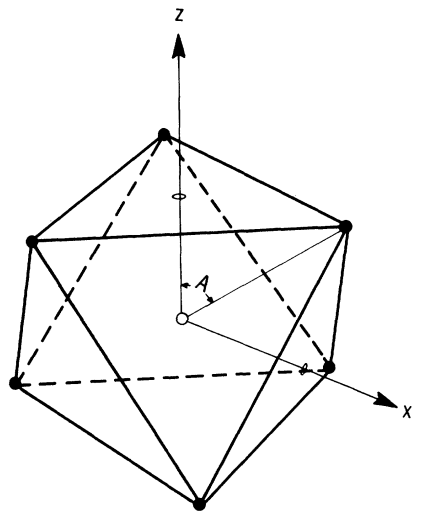

FIG. 7. Coordinate system used for calculating the matrix elements.

the $6d$ states to be degenerate.

Now consider the surroundings of a Pt atom in more detail. There are four similar but nonequivalent Pt sites; around one of them the Sb neighbors are in the positions

$$\pm r'(1, -\alpha, \alpha), \quad \pm r'(\alpha, 1, -\alpha), \quad \pm r'(-\alpha, \alpha, 1),$$

in which

$$r' = r/(1 + 2\alpha^2)^{1/2}, \quad r = \text{Pt-Sb separation},$$

$$\alpha = b/(a - b) .$$

The a is the lattice parameter and $\sqrt{3}b$ is the Sb-Sb separation; $\alpha = 0.316$ for $PtSb_2$; other pyrite structures have very similar values of this parameter. These neighbors lie on an octahedron that is compressed along a [111] axis and rotated about it; the other three Pt sites have equal compressions and rotations about the remaining [111] axes.

To discuss the bonding of the Pt atom we refer to axes (Fig. 7) with the Pt atom as origin, the z axis in a [111] direction, and the x axis such that two of the points of the octahedron lie in the plane $y = 0$. The configuration has threefold symmetry about the z axis, the bonds making azimuthal angles A or $\pi - A$ with the z axis, where

$$\cos A = [3(1 + 2\alpha^2)]^{-1/2} ,$$

$$A \simeq \alpha^2/\sqrt{2} + \cos^{-1}(1/\sqrt{3}) .$$

The distortion of the octahedron is of order α^2, $\simeq 0.1$, which we shall treat as small.

(a) Pt^{2-}: Assume an sp^3d^2 set of orbitals is involved in the bonding. From the threefold rotation and inversion it is readily shown that the possible orthonormal orbitals are

$$\frac{1}{\sqrt{6}}s \pm \frac{1}{\sqrt{2}}\left(\frac{1}{\sqrt{3}}p_z + (\sqrt{\tfrac{2}{3}})p_x\right) + \frac{1}{\sqrt{3}}(c_1 d_{zx} + c_2 d_{x^2-y^2}) \ ,$$

$$\frac{1}{\sqrt{6}}s \pm \frac{1}{\sqrt{2}}\{1/\sqrt{3}\,p_z + (\sqrt{\tfrac{2}{3}})[-\tfrac{1}{2}p_x + (\tfrac{1}{2}\sqrt{3})p_y]\}$$

$$+\frac{1}{\sqrt{3}}\{c_1[-\tfrac{1}{2}d_{zx} + (\tfrac{1}{2}\sqrt{3}\,d_{zy}] + c_2[-\tfrac{1}{2}d_{x^2-y^2} - (\tfrac{1}{2}\sqrt{3}\,d_{xy}]\},$$

$$\frac{1}{\sqrt{6}}s \pm \frac{1}{\sqrt{2}}\left(\frac{1}{\sqrt{3}}p_z + (\sqrt{\tfrac{2}{3}})[-\tfrac{1}{2}p_x - (\tfrac{1}{2}\sqrt{3})p_y]\right)$$

$$+\frac{1}{\sqrt{3}}\{c_1[-\tfrac{1}{2}d_{zx} - (\tfrac{1}{2}\sqrt{3})d_{zy}] + c_2[-\tfrac{1}{2}d_{x^2-y^2} + (\tfrac{1}{2}\sqrt{3})d_{xy}],\}$$

where $c_1^2 + c_2^2 = 1$. The remaining set of nonbonding d orbitals are

$$\psi_1 = (\sqrt{\tfrac{2}{3}})(c_2 d_{zx} - c_1 d_{x^2-y^2}) + \frac{1}{\sqrt{3}}d_{3z^2-r^2} \ ,$$

$$\psi_2 = (\sqrt{\tfrac{2}{3}})\{c_2[-\tfrac{1}{2}d_{zx} + (\tfrac{1}{2}\sqrt{3})d_{zy}]$$
$$- c_1[-\tfrac{1}{2}d_{x^2-y^2} - (\tfrac{1}{2}\sqrt{3})d_{xy}]\} + \frac{1}{\sqrt{3}}d_{3z^2-r^2} \ ,$$

$$\psi_3 = (\sqrt{\tfrac{2}{3}})\{c_2[-\tfrac{1}{2}d_{zx} - (\tfrac{1}{2}\sqrt{3})d_{zy}]$$
$$- c_1[-\tfrac{1}{2}d_{x^2-y^2} + (\tfrac{1}{2}\sqrt{3})d_{xy}]\} + \frac{1}{\sqrt{3}}d_{3z^2-r^2}$$

(on referring back to crystal coordinates, these are the d_{xy}, d_{yz}, d_{zx} harmonics when $\alpha = 0$).

The only parameter available is the ratio c_1/c_2, which we choose to make each bonding orbital stationary in the direction of the bond. If α^2 is small, one finds

$$c_1^2 = \tfrac{2}{3}(1 - 3\alpha^2), \quad c_2^2 = \tfrac{1}{3}(1 + 6\alpha^2) \ .$$

We now evaluate (14) between the nonbonding states and a complete set of $6d$ orbitals, with the result

$$\sigma = \sigma_0[1 - \alpha^2(3\cos^2\theta - 1)] \ , \qquad \text{(A1)}$$

θ being the azimuthal angle of H.

(b) Pt^{4+}: The threefold rotation and orthonormality show that the d_{nb} states must have the same form as derived for Pt^{-2}. Evaluating (14) between the $5d_b$ and $5d_{nb}$ states, one finds

$$\sigma = \sigma_0[1 + \tfrac{3}{2}\alpha^2(3\cos^2\theta - 1)] \ . \qquad \text{(A2)}$$

APPENDIX B: LINE SHAPE IN POWDERS

We here estimate the effect of a small anisotropic line broadening on the powder patterns, assuming that the response of each Pt atom is a Gaussian centered on its resonance frequency, and is characterized by frequency and second moment alone. Following Bloembergen and Rowland,[3] the second moment is taken to be a sum of isotropic exchange and pseudodipole interactions,

$$A^2 = A_0^2[1 + \tfrac{1}{6}\beta\textstyle\sum_n (3\cos^2\theta_{Hn} - 1)^2] \ , \qquad \text{(B1)}$$

in which A_0 is the isotropic broadening, β measures the relative strength of the pseudodipole interaction, θ_{Hn} is the angle between H and the line joining a Pt atom to the nth atom, and the sum is taken over nearest neighbors only. For the time being we take it that the neighbors lie on a regular octahedron; then for small β and with H in the direction (lmn) one has

$$A = A_0\{1 + \tfrac{1}{2}\beta[3(l^4 + m^4 + n^4) - 1]\} \ . \qquad \text{(B2)}$$

We extend Eq. (5) to cover the case in which the resonance field H' is a function of azimuthal angle θ measured from a (111) direction, and the line breadth A is a function of θ and a polar angle ϕ: the response $R(H)$ to an applied field H is

$$R(H) = \frac{1}{2\pi}\int g[H' - H, A(\theta,\phi)]n(H')dH'\,d\phi$$
$$\simeq \int g[H' - H, \bar{A}]n(H')dH'$$
$$+ \frac{1}{2\pi}\int \left[\frac{dg}{dA}\right]_{\bar{A}}[A(\theta,\phi) - \bar{A}]n(H')dH'\,d\phi \ ,$$

where $\bar{A}$ is a suitable mean value of A, $n(H')$ is given above Eq. (5), and g is the derivative with respect to field of a normalized Gaussian:

$$g \sim -\frac{H' - H}{A^3}\,e^{-(H'-H)^2/2A^2} \ .$$

From Eq. (B2)

$$A(\theta,\phi) - \bar{A} = \beta A_0[\tfrac{3}{2}\cos^2\theta - \tfrac{7}{4}\cos^4\theta$$
$$+ \sqrt{2}\,\sin^3\theta\cos\theta\sin 3\phi] \ ,$$

$$\bar{A} = A_0[1 + \tfrac{1}{4}\beta] \ .$$

On using Eq. (3) to give $\cos\theta$ in terms of H' one has

$$R(H) = R_0(H) + \delta R \ ,$$
$$R_0(H) = \textstyle\int_{-W/2}^{W} (H' + \frac{1}{2}W)^{-1/2} g(H - H', \bar{A})\,dH' \ ,$$
$$\delta R = \beta\bar{A}\textstyle\int_{-W/2}^{W}[W^{-1}(H' + \frac{1}{2}W)^{1/2}$$
$$- (7/9W^2)(H' + \tfrac{1}{2}W)^{3/2}]\frac{dg}{dA}\,dH' \ .$$

A convenient property of Gaussians is that $dg/dA = Ad^2g/dH'^2 = -Ad^2g/dHdH'$. The first term in δR is then found as follows:

$$\int (H' + \tfrac{1}{2}W)^{1/2}\frac{dg}{dA}\,dH' = -A\int (H' + \tfrac{1}{2}W)^{1/2}\frac{d^2g}{dHdH'}\,dH'$$

$$= A(H' + \tfrac{1}{2}W)^{1/2}\frac{dg}{dH'} + \tfrac{1}{2}A\frac{d}{dH}\int (H' + \tfrac{1}{2}W)^{-1/2} g\,dH' \ .$$

The last term here is proportional to dR_0/dH, and to first order in β has the effect of shifting R_0 along

the axis of H. Collecting all terms together the end result is

$$R(H) = (1 - 7\beta\bar{A}^2/12W^2)R_0(H + \beta\bar{A}^2/2W) + (3/2W)^{1/2}(\beta/A)\{7(H - W)/6W + \tfrac{1}{6}[1 - (H - W)^2/\bar{A}^2]\}e^{-(H-W)^2/2\bar{A}^2} \quad . \quad \text{(B3)}$$

The last terms are the major part of the correction, the shift and change in magnitude of R_0 being small. The whole correction can be ignored when A is small compared with W, except in the most accurate work, since its major part then affects only the right-hand peak of the powder pattern, and the change is rather small.

The above calculation can be corrected for the effects of the distortion of the octahedron surrounding the Pt atom without much trouble. The effect is to replace the numerical factors $\frac{7}{6}$ and $\frac{1}{6}$ in Eq. (B3) with $\frac{7}{6} + \frac{16}{3}\alpha^2$ and $\frac{1}{6} + \frac{4}{3}\alpha^2$, respectively. This change was made in such a way as to maintain the most convenient experimental definition of β,

$$\beta = (A_{(100)} - A_{(111)})/A_{(111)} \quad .$$

---

[1]D. H. Damon, R. C. Miller, and A. Sagar, Phys. Rev. 138, A636 (1965).

[2]T. P. Das and E. L. Hahn, in *Solid State Physics*, edited by F. Seitz and D. Turnbull (Academic, New York, 1958), Suppl. 1, p. 3ff.

[3]N. Bloembergen and T. J. Rowland, Acta Met. 1, 731 (1953); Phys. Rev. 97, 1679 (1955).

[4]D. W. Feldman, thesis, University of California, Berkeley, 1959 (unpublished).

[5]K. Murakawa, Phys. Rev. 100, 1369 (1955).

[6]The single-crystal line shape for the Pt resonance in $PtSb_2$ is Gaussian – or rather, the derivative of a Gaussian – as best we can determine. The linewidth is anisotropic, the second moment of the line changing from $A^2 = (4.1G)^2$ to $(3.1G)^2$ as H moves from a (100) to a (111) direction (see Appendix B). The use of a single mean line breadth in Eq. (5) fails to give the antimonide powder absorption derivative correctly, it being found that when A is small enough for one to resolve the two peaks on the right of the pattern ($A < 0.4$ W), then the calculated right-hand peak is always the lower of the two (Fig. 5 is not by itself definite; other measurements show that the right-hand peak is always, in fact, higher). Taking the anisotropy of the linewidth into account corrects this discrepancy; the calculated powder pattern is then determined entirely by single-crystal data, apart from its height. In the case of the arsenide σ_0 is the same as in the antimonide, so σ_1 should also be the same as was noted after Eq. (3); this leaves the intrinsic linewidth A as a parameter; the value $A = 1.5$ G gave the calculated points of Fig. 5. The linewidths quoted above are corrected for modulation broadening through the relation $A^2_{\text{Real}} = A^2_{\text{Meas}} - \frac{1}{4}h_m^2$, $2h_m$ being the peak-to-peak modulation amplitude.

[7]E. D. Jones, Phys. Letters 27A, 204 (1968).

[8]R. R. Hewitt and B. F. Williams, Phys. Rev. 129, 1188 (1963).

[9]C. H. Townes and B. P. Dailey, J. Chem. Phys. 17, 782 (1949); see also B. P. Dailey and C. H. Townes, *ibid.* 23, 118 (1955).

[10]R. G. Barnes and W. V. Smith, Phys. Rev. 93, 95 (1954).

[11]N. F. Ramsey, Phys. Rev. 76, 699 (1950); 86, 243 (1952).

[12]L. E. Drain, J. Phys. Chem. Solids 24, 379 (1963).

[13]A. A. Clogston, V. Jaccarino, and Y. Yafet, Phys. Rev. 134, A650 (1964).

[14]R. Freeman, G. R. Murray, and R. E. Richards, Proc. Roy. Soc. (London) 242A, 455 (1957).

[15]R. E. Walstedt, J. H. Wernick, and V. Jaccarino, Phys. Rev. 162, 301 (1967).

[16]R. G. Shulman, J. M. Mays, and D. W. McCall, Phys. Rev. 100, 692 (1955).